

Performance improving of alkali activated blast furnace slag mortars with tile dust

Aylin Özodabaş, Kemalettin Yılmaz

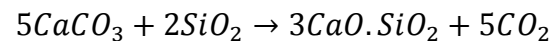
Abstract-- This work investigates the strength development of alkali activated blast furnace slag mortars (AAS) with tile dust (TD) at certain rates. BFS was used instead of cement at the rate of 60% and 80%. Sodium hydroxide (NaOH) and sodium silicate (Na₂SiO₃) alkalis were added as solution into the mixture. First stage Na₂O 6, 7 and 8 wt% of the BFS was added. Better results were obtained from the strength values of the sample containing 8% Na₂O. Because of this result, in the second stage, tile dust was used instead of 5% and 10% of the BFS. However, silicate modules ($M_s = \text{SiO}_2/\text{Na}_2\text{O}$) in both experimental studies were calculated as 0.5, 0.75 and 1.00. Twenty eight-days strength value of AAS+TD (tile dust was used instead of 5% and $M_s=0.75$) specimen are higher than rate of 60% BFS specimen.

Keywords: Blast furnace slag, alkali activator, sodium hydroxide, sodium silicate, tile dust

I. Introduction

The world-wide need to reduce the energy used and the greenhouse gases emitted during cement manufacture has led to the pursuit of more eco-efficient materials, such as alkali-activated slag cements (AAS) [1]. In studies to date, fly ash, metakaolin, blast furnace slag, kaolinitic clays, rice husk, silica fume and red mud were used with AAS concretes. C₃S, C₂S, C₃A and C₄AF. These systems serve their purpose well but have some drawbacks. The synthesis of high CaO minerals involves large fuel and energy consumption.

Because Portland cement and the concrete derived from it constitute the largest volume manufactured material in the world, it is a significant source of carbon dioxide. This is the result of the decarbonation of limestone in the kiln during manufacturing and the use of fossil fuel in the kiln.



The production of 1 ton of Portland cement accounts for 1 ton of CO₂ [2].

These cements are obtained by mixing vitreous granulated blast furnace slag with highly basic solutions such as waterglass (Na₂O·nSiO₂·mH₂O+ NaOH), NaOH or Na₂CO₃, among others. In terms of mechanical properties, AAS cements are comparable to OPC, particularly when waterglass is used as the activating solution [3, 4].

This slag produced from industrial by-products requires less production energy than ordinary Portland cement. Many valuable research results on this material have been reported. Alkali activated slag concrete (AASC) has been found to have some superior properties compared to ordinary Portland cement concrete (OPCC), namely, a high early strength and excellent durability in an aggressive environment (exposed to acid, sulfate or seawater). Many alkali activated slag properties have been explored [5–8].

Collins and Sanjayan reported that micro cracks in AAS concrete increased from the lack of curing moisture. A survey of the published literature showed that this is new binder system has some serious problems such as rapid setting and high drying shrinkage [9–11].

Sintered red clay ceramic is used to produce hollow bricks which are manufactured in enormous quantities in Spain. They also constitute a major fraction of construction and demolition waste. The aim of this research was to investigate the properties and microstructure of alkali-activated cement pastes and mortars produced using red clay brick waste. The work shows that the type and concentration of alkali activator can be optimised to produce mortar samples with compressive strengths up to 50 MPa after curing for 7 days at 65 °C. This demonstrates a new potential added value reuse application for this important waste material [12].

Red clay brick waste originating primarily from demolished brick walls represents approximately 54 wt.% of construction and demolition waste in Spain [13]. As previously reported [14], almost 30 million tons of structural ceramics and 608 millionm² of tiles were manufactured by the Spanish ceramics industry in 2006. According to Pacheco-Torgal and Jalali [15].

I. Experimental Program

A. Materials

Tile or brick dust that obtains as a result of waste dust occurs in tile production. There are many tile factories in Turkey. Tile dust is a pozzolanic material.

Ground granulated blast furnace slag (GGBFS) has been used for many years as a supplementary cementitious material in concrete technology. The slag is a by-product material obtained from the manufacturing of pig iron in the blast furnace and is formed by a combination of the earthy constituents of iron ore with limestone flux. There are various uses of ground granulated blast furnace slag as a binding material, and it can be used as a mineral admixture in concrete production. [16].

The alkaline activators sodium hydroxide and sodium silicate with Ms = 0.5, 0.75 and 1.00 were used for this study. The amount of Na₂O was 8 wt% of the slag (BFS).

Mortars with a binder:sand ratio of 1:3 and a water/binder ratio of 1:2 were used. Blast furnace slag (BFS) was used instead of cement at 60 wt% and 80 wt%. In the second stage, tile dust was added instead of BFS 5 wt% and 10 wt%. Produced specimens were cured at 7, 28 and 90 days, and their flexural and strength values were examined (see Figs. 1–6).

The chemical composition and properties of the Ordinary Portland Cement (CEM I), blast furnace slag and clay (used for making tiles) used are tabulated in Table 1. Mortar specimen values are also given in Tables 2 and 3.

TABLE I. CHEMICAL COMPOUND

Chemical Composition (%)	Clay	OPC	BFS
SiO ₂	50.60	20.35	39.18
Al ₂ O ₃	14.95	5.98	9.81
TiO ₂	0.67	-	-
Fe ₂ O ₃	7.88	3.06	1.90
CaO	7.40	63.35	32.52
MgO	4.26	1.89	9.94
K ₂ O	2.50	0.88	1.50
Na ₂ O	-	0.58	0.40
SO ₃	-	2.89	-
Specific gravity (g/cm ³)	1	3.10	2.53

B. Mortar Preparation

AAS mortars, which were prepared with OPC, pumice and standard sand, were determined by Turkish standard (TS EN 196-1)

Prismatic specimens (40 x 40 x 160 mm) from each mixture underwent a flexural strength test according to the Turkish standard. The specimens were loaded from their mid-span. The compressive strength tests were conducted following the flexural tests on the two broken pieces according to Turkish standard. The compressive strengths of the specimens were measured after 7, 28 and 90 days, as specified in Turkish standard

II. Results

The results show that the flexural and compressive strength values changed according to the different types and dosages of activators.

A. Flexural And Compressive Strength

In this study, two stages were conducted sequentially. In the first stage, the influence of the dosage of sodium silicate and sodium hydroxide on the compressive strength was studied. Keeping the liquid/slag ratio constant, the alkali modules and the total activator dosage were taken into account. The experimental results revealed the total activator dosages [17]. Figure 1, 2 and 3 shows that the value of the 50BFS+10TD $M_s=1.00$ content has a better result than the other specimens; 7, 28 and 90 days flexural strength values. For this reason, the value of 8% Na_2O was used in second stage, and tile dust was added to improve durability. Figure 4, 5 and 6 shows that the value of the 70BFS+10TD $M_s=0.75$ content has a better result than the other specimens; 7, 28 and 90 days compressive strength values.

TABLE II. THE 7, 28 AND 90 DAYS FLEXURAL STRENGTH VALUES OF THE TILE DUST MIXED SPECIMENS

Mixture (%)	7Days (MPa)	28Days (MPa)	90Days (MPa)
60 BFS ^a	3.53	5.70	7.28
55BFS+5TD ^b	3.07	5.61	6.77
55BFS+5TD $M_s=0.5$	4.75	5.71	5.26
55BFS+5TD $M_s=0.75$	4.69	5.76	5.72
55BFS+5TD $M_s=1.00$	5.79	6.45	6.21
50BFS+10TD ^b	4.03	5.77	7.11
50BFS+10TD $M_s=0.5$	4.95	5.43	5.67
50BFS+10TD $M_s=0.75$	5.01	5.85	6.31
50BFS+10TD $M_s=1.00$	6.34	6.63	6.60
80 BFS ^a	3.06	4.58	7.44
75BFS+5TD ^b	1.77	4.75	5.94
75BFS+5TD $M_s=0.5$	4.59	5.59	5.57
75BFS+5TD $M_s=0.75$	5.14	6.50	6.19
75BFS+5TD $M_s=1.00$	2.53	3.42	3.74
70BFS+10TD ^b	2.54	4.51	6.18
70BFS+10TD $M_s=0.5$	4.72	5.52	5.29
70BFS+10TD $M_s=0.75$	5.75	6.80	5.93
70BFS+10TD $M_s=1.00$	1.86	3.28	3.29

^a Reference specimens.

^b Non alkali activated tile dust samples.

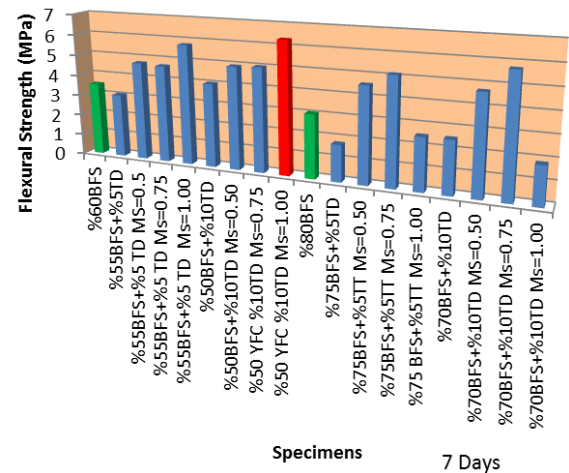


Figure1. A graph of the flexural strength of the tile dust content specimens at 7 days

TABLE III. THE 7, 28 AND 90 DAYS COMPRESSIVE STRENGTH VALUES OF THE TILE DUST MIXED SPECIMENS

Mixture (%)	7Days (MPa)	28Days (MPa)	90Days (MPa)
60 BFS ^a	13.94	32.25	40.70
55BFS+5TD ^b	14.62	27.70	34.80
55BFS+5TD $M_s=0.5$	15.90	23.15	30.00
55BFS+5TD $M_s=0.75$	16.38	27.15	37.00
55BFS+5TD $M_s=1.00$	18.18	26.55	37.40
50BFS+10TD ^b	15.02	30.05	41.05
50BFS+10TD $M_s=0.5$	15.58	22.85	28.50
50BFS+10TD $M_s=0.75$	16.46	27.50	39.90
50BFS+10TD $M_s=1.00$	18.11	27.20	39.70
80 BFS ^a	11.20	17.88	32.05
75BFS+5TD ^b	6.65	18.73	27.70
75BFS+5TD $M_s=0.5$	14.70	24	35.15
75BFS+5TD $M_s=0.75$	23.40	35.85	47.65
75BFS+5TD $M_s=1.00$	14.67	19.54	22.50
70BFS+10TD ^b	7.32	19.02	27.45
70BFS+10TD $M_s=0.5$	15.21	24.10	35.05
70BFS+10TD $M_s=0.75$	22.90	36.25	46.75
70BFS+10TD $M_s=1.00$	9.50	14.85	19.06

^a Reference specimens.

^b Non alkali activated tile dust samples.

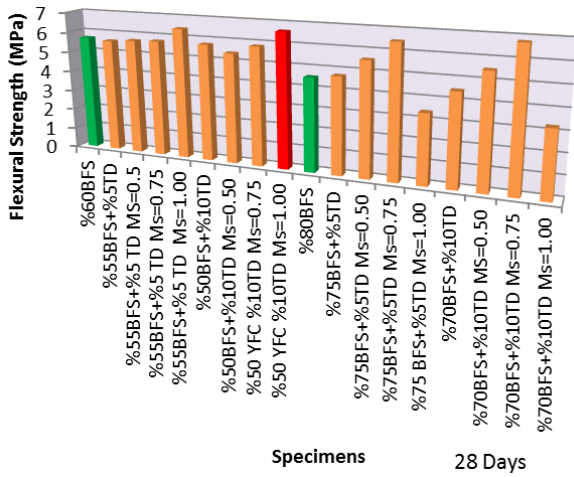


Figure2. A graph of the flexural strength of the tile dust content specimens at 28 days

When the compressive strengths as a function of the activator M_s for a given value are considered, different trends emerge for early and later ages. All of the samples' compressive strength values increased for 7 days and only slightly increased after 28 and 90 days. Furthermore, the values were close to each other.

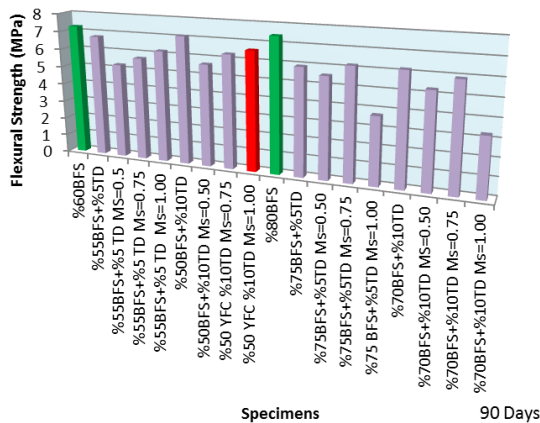


Figure3. A graph of the flexural strength of the tile dust content specimens at 90 days

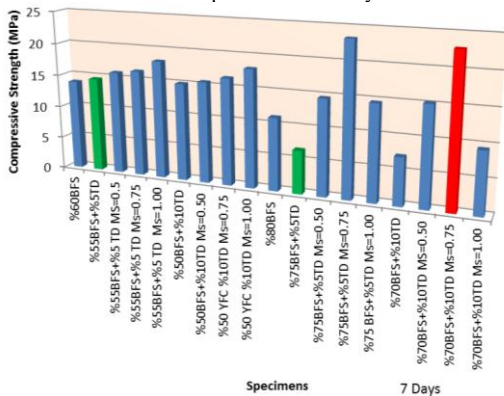


Figure4. A graph of the compressive strength of the tile dust content specimens at 7 days

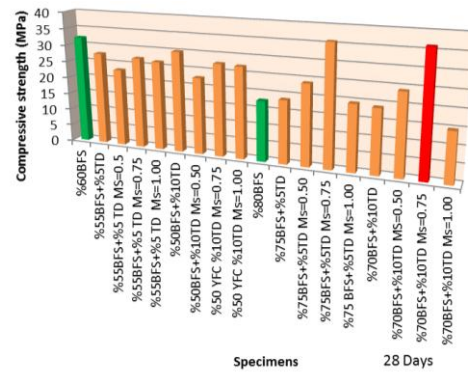


Figure5. A graph of the compressive strength of the tile dust content specimens at 28 days

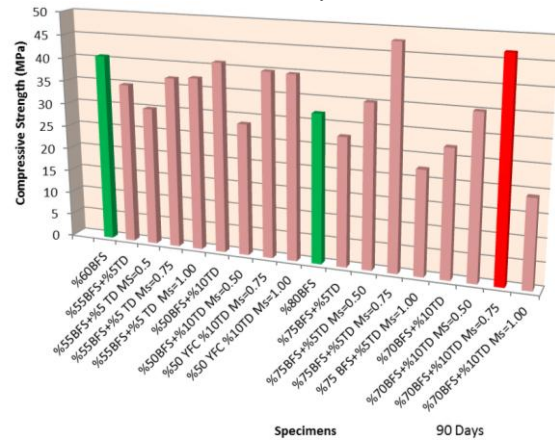


Figure6. A graph of the compressive strength of the tile dust content specimens at 90 days

iii. Discussion

A. Microstructure Investigations

SEM studies were conducted to provide a visual insight into the microstructure and mineralogical composition of the samples [18]. Different proportions of the samples were produced, and the microstructure of the mortars was investigated with SEM analysis after 90 days in water. In figure 7 samples had a denser and porous matrix. In figure 8, drying shrinkage cracks are visible. Previous studies have reported that the dry shrinkage of liquid sodium silicate activated slag mortar increases with an increase in the sodium concentration for a constant SiO_2/Na_2O ratio [19]. Highly crystalline calcite was observed for the AAS samples, consistent with its high CaO content (Fig. 7). In Fig. 9, the mortar mixture presented has a low magnification ratio. In addition to the dense structure of the matrix, global air gaps can be seen. The binding property of the C-S-H ($CaO.SiO_2.H_2O$) structure improves with a decrease in the Ca/Si ratio [20].

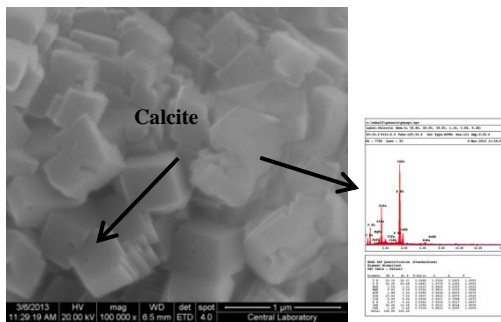


Figure.7. SEM micrographs of the 55% BFS+5% TD $M_S = 0.50$ sample with 8% Na_2O – 5000x.[25]

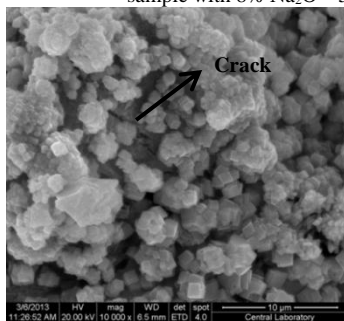


Figure8. SEM micrographs of the 55% BFS+5%TD $M_S = 0.50$ sample with 8% Na_2O – 10.000x

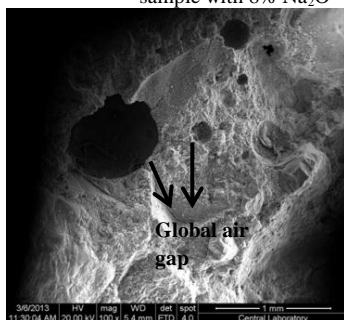


Figure9. SEM micrographs of the 40% BFS $M_S = 0.75$ sample with 8% Na_2O – 100x

iv. Conclusions


This study aimed at investigating the mechanical properties AAS+TD mortars with various dosages of alkali activated solution. The main conclusions extracted from the present study are the following;

The maximum compressive strength values of 75BFS+5TD $M_S=0.75$ and 70BFS+10TD $M_S=0.75$, 23.40-35.85-47.65 MPa and 22.90-36.25-46.75MPa were obtained in 7, 28 and 90 days. These results are consistent with the low cement ratio and improved compressive strength presented by the specimens alkali-activated with sodium silicate and sodium hydroxide. The compressive strength increases as the amount of blast furnace slag increased. However, higher silicate modules contents increased the mortar viscosity and reduced setting time.

References

- [1] F. Puertas, M. Palacios, A. Gil-Maroto, T. Vázquez. Alkali-aggregate behaviour of alkali-activated slag mortars: Effect of aggregate type. *Cement Concr Comp* 2009;31:277–284.
- [2] Roy DM. Alkali-activated cements: opportunities and challenges. *Cem Concr Res* 1999;29(2):249–54.
- [3] Bakharev T, Sanjayan JG, Cheng Y-B. Sulfate attack on alkali-activated slag concrete. *Cement Concr Res* 2002;32:211–6.
- [4] Bakharev T, Sanjayan JG, Cheng Y-B. Resistance of alkali-activated slag concrete to acid attack. *Cement Concr Res* 2003;33:1607–11.
- [5] Roy DM, Idorn GM. Hydration, structure, and properties of blast furnace slag cements, mortars, and concrete. *ACI Mater J* 1982;79(12):444–57.
- [6] Pu XC, Gan CC, Wang SD, Yang CH. Summary reports of research on alkaliactivated slag cement and concrete. Chong-qing, China: Chongqing Institute of Architecture and Engineering; 1988.
- [7] Glukhovskiy VD. Slag-alkali concretes produced from fine-grained aggregate. Vishcha Shkola, Kiev: USSR; 1981.
- [8] Glukhovskiy VD, Pakhomov VA. Slag-alkali cements and concretes. Kiev: Buidivelnik Publishers; 1978.
- [9] Collins F, Sanjayan JG. Cracking tendency of alkali-activated slag concrete subjected to restrained shrinkage. *Cem Concr Res* 2000;30(5):791–8.
- [10] Gong C, Yang N. Effect of phosphate on the hydration of alkali activated red mud–slag cementitious material. *Cem Concr Res* 2000;30(7):1013–6.
- [11] Collins F, Sanjayan JG. Effect of pore size distribution on drying shrinkage properties of alkali-activated slag concrete. *Cem Concr Res* 2000;30(9):1401–6.
- [12] Reig L, Tashima M.M, Borrachero M.V, Monzó J, Cheeseman C.R, Payá J. Properties and microstructure of alkali-activated red clay brick waste. *Constr Build Mater* 2013;43 98–106
- [13] Ministerio de Fomento de España. Actualización del catálogo de residuos utilizables en construcción; 2010. p. 123–158.
- [14] Reig L, Tashima MM, Soriano L, Borrachero MV, Monzo J, Paya J. Alkaline activation of ceramic waste materials. *Waste Biomass Valor* 2013. <http://dx.doi.org/10.1007/s12649-013-9197-z>.
- [15] Pacheco-Torgal F, Jalali S. Reusing ceramic wastes in concrete. *Construct Build Mater* 2010;24(5):832–8.
- [16] Müdüroğlu M., Atak S. Investigation of Characteristics of Clay Building Material Used in Roofing tile. 3. Symposium on Industrial Raw Materials. 14-15 October 1999, Izmir, Turkey.
- [17] Chang JJ. A study on the setting characteristics of sodium silicate-activated slag pastes. *Cement Concr Res* 2003;33:1005–11.
- [18] Cihangir F, Ercikdi B, Kesimal A, Turan A, Deveci H. Utilisation of alkali-activated blast furnace slag in paste backfill of high-sulphide mill tailings: Effect of binder type and dosage. *Minerals Engineering* 2012;30: 33–43
- [19] Özodabaş A, Yılmaz K., Improvement of the performance of alkali activated blast furnace slag mortars with very finely ground pumice. *Constr Build Mater* 48 (2013) 26–34
- [20] Chi M. Effects of dosage of alkali-activated solution and curing conditions on the properties and durability of alkali-activated slag concrete. *Constr Build Mater* 2012;35:240–5.

About Author (s):

	<p>Aylin Özodabaş Assitant Professor (PhD) Research areas: Concre Technology, sustainable concretes characterization techniques applied</p>
	<p>Kemalettin Yılmaz Professor (PhD) Research areas: Concrete Technology, fibrated concretes characterization techniques applied</p>